AD-A095 667 NAVAL RESEARCH LAB WASHINGTON DC F/G 20/9
CHARACTERISTICS OF ABLATION PLASMA FROM PLANAR, LASER-DRIVEN TA--ETC(U)
MAR 81 J GRUN, R DECOSTE, B H RIPIN

UNCLASSIFIED NRL-MR-4410 NL

END
DATE FILMED
3-81
DTIC

(14) NRL-MR-4410

SECURITY CLASSIFICATION OF THIS PAGE (When Data Entered)

REPORT DOCUMENTATION PAGE

READ INSTRUCTIONS BEFORE COMPLETING FORM

1. REPORT NUMBER: NRL Memorandum Report 4410	2. GOVT ACCESSION NO.: AD-A095667
3. RECIPIENT'S CATALOG NUMBER:	
4. TITLE (and Subtitle): CHARACTERISTICS OF ABLATION PLASMA FROM PLANAR, LASER-DRIVEN TARGETS.	5. TYPE OF REPORT & PERIOD COVERED: Interim report on a continuing NRL problem.
	6. PERFORMING ORG. REPORT NUMBER:
7. AUTHOR(s): (10) J. Grun* R. Decoste† B. H. Ripin and J. Gardner	8. CONTRACT OR GRANT NUMBER(s):
9. PERFORMING ORGANIZATION NAME AND ADDRESS: Naval Research Laboratory, Washington, D. C. 20375	10. PROGRAM ELEMENT, PROJECT, TASK AREA & WORK UNIT NUMBERS: 47-0859-0-1
11. CONTROLLING OFFICE NAME AND ADDRESS: U. S. Departmentof Energy, Washington, D. C. 20545 (11) 9	12. REPORT DATE: March 1981
	13. NUMBER OF PAGES: 16
14. MONITORING AGENCY NAME & ADDRESS (if different from Controlling Office) (12) 17	15. SECURITY CLASS. (of this report): UNCLASSIFIED
	15a. DECLASSIFICATION/DOWNGRADING SCHEDULE:

16. DISTRIBUTION STATEMENT (of this Report)

Approved for public release; distribution unlimited.

17. DISTRIBUTION STATEMENT (of the abstract entered in Block 20, if different from Report)

Accession For	
NTIS GRA&I	X
DTIC TAB	☐
Unannounced	☐
Justification	
By	
Distribution/	
Availability Codes	
Dist	Avail and/or Special
A	

18. SUPPLEMENTARY NOTES

*Mission Research Corporation, Alexandria, VA.
†Institut de Recherche d'Hydro-Quebec, Varennes, Quebec Canada.

19. KEY WORDS (Continue on reverse side if necessary and identify by block number)

Ablation parameters
Ablation pressure
Mass ablation rates
Spot-size effects
Laser-plasma interaction
Ablation velocity
Ballistic pendulum

20. ABSTRACT (Continue on reverse side if necessary and identify by block number)

The momentum, energy, and velocity characteristics of plasma ablating from planar targets irradiated by long Nd-laser pulses (4-nsec, $< 10^{14}$ W/cm^2) are measured and the dependence of ablation parameters upon absorbed irradiance is determined. Large laser spots are used in these experiments so that the results are not sensitive to boundary effects.

DD FORM 1 JAN 73 1473 EDITION OF 1 NOV 65 IS OBSOLETE
S/N 0102-LF-014-6601

251950

SECURITY CLASSIFICATION OF THIS PAGE (When Data Entered)

CHARACTERISTICS OF ABLATION PLASMA FROM PLANAR, LASER-DRIVEN TARGETS

Considerable effort is underway to study the feasibility of imploding moderate aspect ratio, high gain fusion pellets. In this concept, long duration laser or ion beam pulses ablate pellet surface material whose rapid evaporation creates a pressure that implodes the pellet walls. This pressure, and the speed of the ablated material or the mass ablation rate, help determine the velocity of the imploding walls, their rate of acceleration and the hydrodynamic efficiency of the implosion. Knowledge of these ablation parameters is basic to the calibration of computational codes used to design a fusion pellet, and is basic to the search for an irradiance regime consistent with a stable and efficient implosion. We present here the magnitudes and scalings with absorbed irradiance of the ablation pressure, the ablation velocity, and the mass ablation depth (∝ mass ablation rate). Our measurements utilize planar foil targets. Large diameter laser-spots and uniformly irradiated disks are used so that the results are not sensitive to focal-spot edge effects associated with energy flow thru the focal-spot periphery.

Configuration of the experiment is similar to one previously described.[1] Polystyrene (CH) targets are irradiated by a 1.05 μm wavelength, 4-nsec FWHM duration laser pulse focused thru an f/6 aspheric lens to an average irradiance $\lesssim 10^{14}$ W/cm^2. The pulse length is long enough so that stationary ablation physics dominate the laser plasma interaction.[2] The ablation parameters are inferred from angular distributions of the ablation plasma energy, velocity, and momentum measured with arrays of plasma calorimeters, time-of-flight ion collectors, and ballistic pendula

Manuscript submitted January 7, 1981.

arranged around the target. Although any two of the measured quantities would have been sufficient, we measured all three with independent diagnostics to verify the self-consistency of our results. The pendula employed here were tested and calibrated in the experimental environment. We verified that pendulum recoil is caused by plasma impact only and that the pendulum array balances blowoff plasma and recoiling target momenta (to within 30%). We discovered, however, that material reflected or sputtered from the pendulum surface affects the pendulum response. Therefore, plasma momentum determined using the common bench calibration of the pendulum would overestimate the true plasma momentum by a factor of 2.4 ± 0.6. To determine the contribution of material reflection or sputter to the absolute calibration, we built a double-pendulum device. It consists of a primary pendulum directly facing the blowoff plasma and a secondary pendulum oriented to detect most of the material reflected or sputtered from the primary pendulum but shielded from the blowoff plasma. Details of this calibration are given elsewhere.[3]

To model the surface of large spherical pellets we utilize wide foil targets irradiated by large, 1-mm diameter laser spots. The targets are sufficiently thick so that their motion has little effect on the measurements. In some cases we also use uniformly irradiated disks.[4] These disks have two advantages over foil targets: first, the laser-target interaction area A that enters into calculations of absorbed irradiance, ablation pressure, and mass ablation depth is well known; second, any energy that escapes the interaction area is easily measured and its effect

on the results easily estimated. A small loss of ablation plasma energy to the rear of disk targets does occur, but this has minimal effect on the ablation parameters. For example, for 300 μm and 600 μm diameter disks less than 20% of the total absorbed (plasma and target) energy reaches the rear disk surface, while for 1000 μm and 1200 μm diameter disks less than 5% of the absorbed energy reaches the rear disk surface. At the irradiances employed here, this excess energy is probably due to the flow of hot thermal plasma around the disk edges: Very energetic suprathermal electrons[5] are not the dominant mechanism as evidenced by the low level x-ray emission observed above 20 keV.[6]

Fig. 1 shows angular distributions of the ablation plasma energy $E(\theta)$, momentum $p(\theta)$, and velocity $\bar{u}(\theta)$; $\bar{u}$ is a mean velocity unfolded from highly peaked ion-collector traces, typical of steady state ablation, assuming a constant charge state and secondary electron coefficient. The angular distributions are set mainly by the nozzle-like flow of collisional plasma near the target surface and also somewhat by the thermal expansion of the plasma once it becomes collisionless.[7] This is consistent with our observation that the shapes of distributions from various diameter (0.3 to 1.2 mm) disks and wide foils irradiated by various diameter laser-spots (0.3 to 2 mm) are similar. The momentum angular distribution, for example, is characterized by a half cone angle $\cos^{-1}(P_\perp/P) = 40^\circ$ for both the disk and wide foil cases; $P_\perp$ is the normal component of the total momentum P calculated by integrating the momentum distribution $p(\theta)$ or the

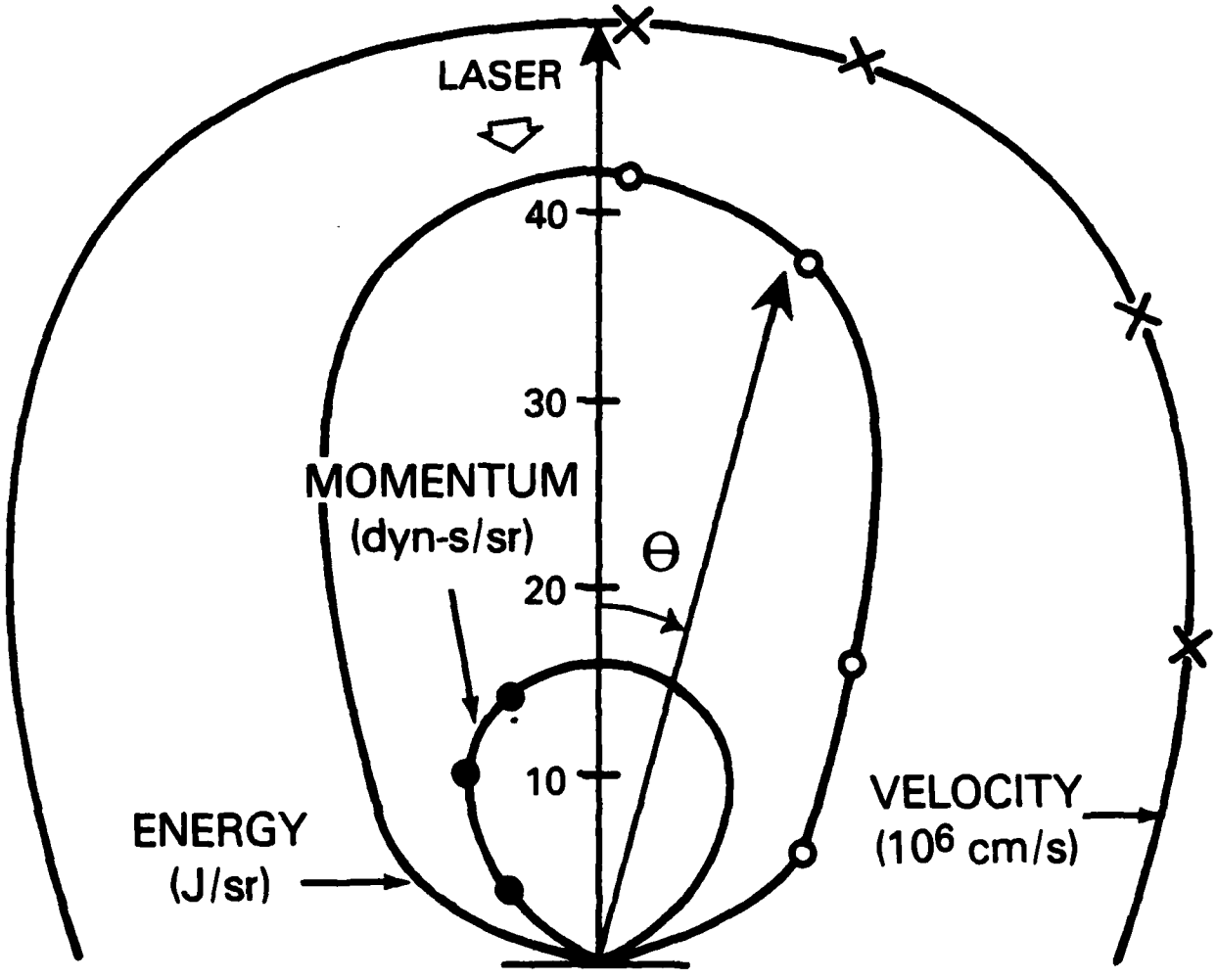

Fig. 1 — Distribution of ablation velocity, energy, and momentum measured with time-of-flight detectors, plasma calorimeters, and ballistic pendula respectively. The target is a 1.2 mm diameter CH disk irradiated at $3 \times 10^{12} W/cm^2$.

distribution of $2E/\bar{u}$ over all solid angles. We use distributions such as those in Fig. 1 to infer ablation pressure, $\mathcal{P}_\perp \equiv P_\perp/\tau A$, ablation mass m_a, mass ablation depth $d \equiv m_a/\rho A$, mass ablation rate $\dot{m}_a \equiv \rho A d/\tau$, and the ablation velocity normal to the target surface $u_\perp \equiv P_\perp/m_a$. Here, τ and ρ are the laser pulse duration and target density respectively.

Fig. 2a shows the scaling of ablation pressure with absorbed irradiance[8] to be $\mathcal{P}_\perp \propto I_a^{0.8}$ for disks and wide foil targets. Momentum in the case of disk targets is determined in two independent ways: first directly, using the pendulum array (dark markers) and second indirectly, using energy and velocity data (open markers); wide foil results (X) use the latter method only. Agreement between the two methods increases our confidence in the results. The scalings with absorbed irradiance of the ablation velocity, $u_\perp \propto I_a^{0.2}$, and the mass ablation depth, $d \propto I_a^{0.6}$, are shown in Fig. 2b.

The measured ablation parameters agree well with like quantities calculated using a one-dimensional (planar geometry), single temperature hydrodynamic code (Fig. 2). This code is a sliding zone Eulerian FCT code that requires no artificial viscosities, utilizes classical thermal transport physics with no ad-hoc inhibition, and uses the same irradiance profile as the experiment. Absorption is by inverse-bremsstrahlung in the underdense region with any remaining laser energy dumped smoothly into two zones surrounding the critical surface. To make a direct comparison with our data, we calculate the momentum and mass of all plasma

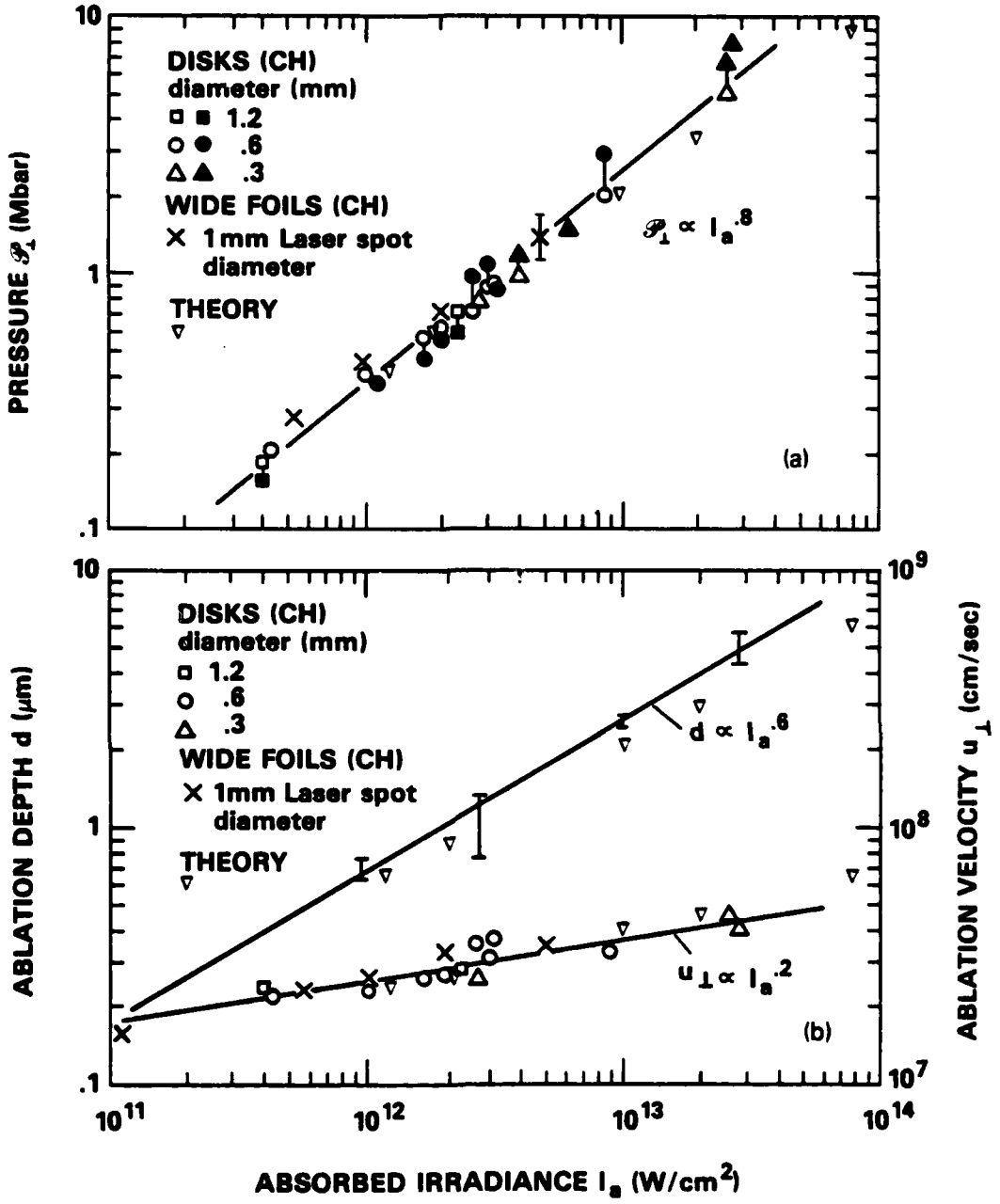

Fig. 2 — (a) Ablation pressure versus absorbed laser irradiance for disks and wide foil targets. The data denoted by ■,●,▲ are inferred using momenta measured with ballistic pendula. The data □,○,△ are obtained using calorimeter and time-of-flight measurements. The symbol ▽ denotes theoretical results. (b) : Mass ablation depth d and normal ablation velocity $u_\perp$ versus absorbed irradiance I_a.

moving toward the laser after these quantities reach their asymptotic values (14 nsec after the laser pulse peak), and determine the temporally averaged ablation parameters $\mathcal{P}_\perp$, d, $u_\perp$ in the same manner as the experiment. (Peak calculated pressures which occur near the ablation surface are only 20% higher than the temporally averaged calculated pressures.) The good agreement between measured and calculated ablation parameters supports the view that basic conservation laws without any transport inhibition govern laser-target interaction physics in this irradiance and laser-pulse length regime.

As we have already shown, the flow characteristics of ablation plasma from planar targets are set by its nozzle-like expansion from the target surface. Thus, plasmas from planar targets are not truly one-dimensional. The good agreement between our experiment and a one-dimensional, planar geometry, code may be explained, however, if the final nature of the ablation parameters is determined near the target surface, when the plasma flow is still planar. This picture is born out by the code which shows that most of the ablation plasma acceleration occurs between the ablation surface and a few times the distance from the ablation surface to the critical surface. This ablation surface to critical surface separation is about 0.1mm at 1×10^{13} W/cm^2 (and less at lower irradiance) which is smaller than the laser-spot diameters in the experiment. One-dimensional, spherical calculations with a large ratio of pellet radius (0.5 cm) to ablation to critical-surface distance gave irradiance scaling laws similar to those in planar geometry.

We also verified that our pressures, determined from asymptotic measurements, are the same (within 30%) as the ablation pressures deduced from measurements of target acceleration.[3,9]

Studies using flat targets are subject to criticism that phenomena at the focal-spot periphery distort effects ascribed to the spot as a whole. Such phenomena may include energy leakage laterally across the focal-spot edge which alters the irradiance distribution, and extraneous plasma from target areas outside the focal spot which contributes to the measured results. To check for these effects we placed planar targets in the near field of the focusing lens and varied the spot-size by aperturing the laser beam while monitoring the ablation velocity. Because of laser energy limitations, this experiment used an average irradiance of 1×10^{12} W/cm^2. But even at this low irradiance, the ablation velocity does vary with spot size (Fig. 3a). The variation is small, however, if the laser spot diameter is sufficiently large ($\geq$1 mm). That is why experiments on foils reported here utilize large laser spots, even though this lowers the maximum irradiance achievable with our laser. It is also clear that controlling irradiance by changing the focal-spot size, as is often done, may lead to misleading results.

Two parameters which may change the effective spot size are the spatial profile of the incident irradiance and the lateral heat flow thru the focal spot periphery. Since the number of ions at a particular velocity depends on absorbed irradiance, both these phenomena may contribute to the velocity variation in Fig. 3a. Lateral heat flow especially could shift energy from

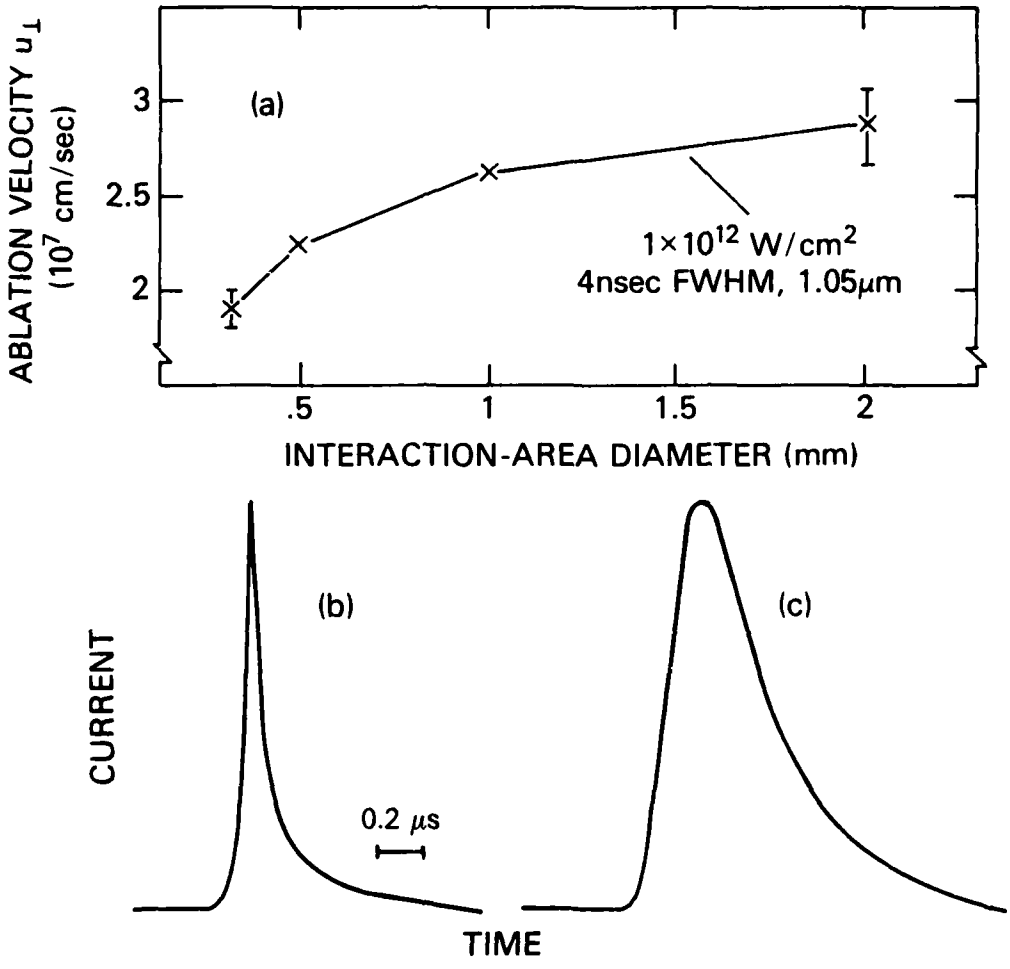

Fig. 3 — (a) Ablation velocity $u_\perp$ vs. interaction-area diameter for wide foil targets. (Interaction-area is defined as the area that contains 90% of the incident laser energy.) (b), (c) Examples of very narrow and broad charge collector traces. The collectors are 28 cm from the target at 2° to its normal.

a higher to a lower portion of the effective irradiance profile and increase the fraction of low velocity ions. Larger spot sizes, with a relatively uniform and flat topped illumination, have a smaller fraction of absorbed energy escaping thru their edges and, therefore, behave somewhat independently of spot size diameter.

Finally, we make this observation: Stationary ablation plasmas produce very mono-energetic ions.[2,10] In experiments, however, non-uniform irradiation, temporal variation of the laser beam, or heat flow thru the focal-spot periphery may broaden ion velocity distributions. In most of our cases ion velocity distributions are highly peaked with a peak velocity to FWHM ratio of 3:1. Nevertheless, under some experimental conditions even narrower distributions (peak velocity: FWHM = 7:1 - see Fig. 3b) and broader distributions (peak velocity: FWHM = 2:1 - see Fig. 3c) are observed. We note that generally; small diameter disks produce narrower distributions than large diameter disks, disk targets produce narrower distributions then foil targets, and small laser-spots produce narrower distributions then large laser spots. Also, the velocity spread of the most highly peaked cases is consistent with that expected for temporal variation in the laser beam alone.[11] We attempted to determine whether spatial irradiance profiles alone are responsible for the broadening of the distributions by using masks placed in the beam to alter the irradiance profile and using disk targets of various diameters to intercept different parts of the laser beam. Our results were inconclusive.

In summary, we studied the ablation characteristics of plasma from planar, laser driven targets. We found that ablation pressure, ablation velocity, and mass ablation depth scale as the 0.8, 0.2 and 0.6 power of the absorbed irradiance. Our results agree well with a one-dimensional hydrodynamic code that uses classical transport physics. Pressures of 10 Mbar exist at 5×10^{13} W/cm^2. Hydrodynamically efficient compression of moderate aspect ratio pellets at this or slightly higher irradiance may thus be possible. We also found that due to edge-effects ablation velocity varies with laser-spot size; but the variations are small for sufficiently large spots.

We thank S.P. Obenschain, S.E. Bodner, C. Manka, and H. Griem for valuable discussions. The technical assistance of N. Nocerino, E. Turbyfill, M. Fink, L. Seymour and R. McGill is greatly appreciated. This work was supported by the U.S. Department of Energy and Office of Naval Research.

REFERENCES

(*) Present address: Mission Research Corporation, Alexandria, VA. Work performed while associated with the Dept. of Physics, University of Maryland, College Park, MD.

(†) Present address: Institut de Recherche d'Hydro-Quebec Varennes, Quebec, JOL 2PO, Canada. Work performed while associated with the Sachs Freeman Corporation.

1. A description of these studies up to 1979 is given by: B.H. Ripin, et al. Phys. Fluids 23, 1012 (1980).
2. M.K. Matzen and R.L. Morse, Phys. Fluids 22, 654 (1979).
3. J. Grun, Ph.D. Dissertation, University of Maryland (1981), unpublished.
4. Intensity variations are ±50%.
5. N.A. Ebrahim, C. Joshi, D.M. Villeneuve, N.H. Burnett, and M.C. Richardson, Phys. Rev. Lett. 43, 1996 (1979).
6. F. Young, private communication.
7. M.J. Herbst and J. Grun, NRL Memo 4436, 1980, submitted for publication.
8. B. Arad, S. Eliezer, Y. Gazit, H.M. Loebenstein, A. Zigler, H. Zmora, and S. Zweigenbaum, J. Appl. Phys. 50, 6817 (1979).
9. S.P. Obenschain, J. Grun, B.H. Ripin, and E.A. McLean, submitted for publication.
10. J.P. Anthes, M.A. Gusinow, and M.K. Matzen, Phys. Rev. Lett. 41, 1300 (1978).

11. We assume that the time and space averaged scalings of Fig. 2b also apply at each point in time. Then, $dN \propto I^{0.6}(t)\,dt$ and $u \propto I^{0.2}(t)$, where I, N, u, t are the irradiance, number of ions, ion velocity, and time respectively. Note that a Maxwellian fit to the narrower ion traces (Fig. 3b) infers an $\sim$100 eV ion energy spread; the actual ion temperature is smaller since temporal variations can account for most of the spread. The ion temperature is probably fixed at a higher density than that at which the $\sim$300 eV electron-temperatures are derived from x-ray Bremsstrahlung.

DISTRIBUTION LIST

NRL, Code 4730 (110 copies) NRL, Code 4700 (25 copies)

USDOE
Division of Laser Fusion
Washington, D.C. 20545
Attn: Dr. G. Canavan
Dr. R. Schreiver
Dr. O. Lewis

Lawrence Livermore Laboratory
P.O. Box 808
Livermore, CA 94551
Attn: Dr. J. Emmett
Dr. J. Holzrichter
Dr. W. Simmons
Dr. J. Nuckolls

Schaefer Assoc.
1901 N. Fort Meyer Drive
Arlington, VA 22211
Attn: Dr. E. Gerry

Defense Technical Information Center (12 copies)
Cameron Station
5010 Duke Street
Alexandria, VA 22314

Science Applications Inc.
Crystal City, VA
Attn: Dr. W. Sooy

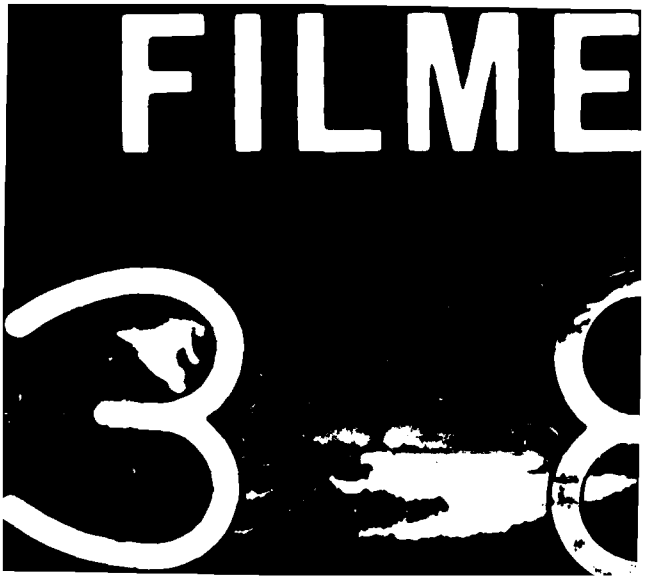
FILME